Vision Res. Vol. 29, No. 11, pp. 1539–1559, 1989
Printed in Great Britain. All rights reserved

0042-6989/89 $3.00 + 0.00

ROD FLICKER PERCEPTION: SCOTOPIC DUALITY, PHASE LAGS AND DESTRUCTIVE INTERFERENCE

LINDSAY T. SHARPE,[1]* ANDREW STOCKMAN[2] and DONALD I. A. MACLEOD[2]
[1]Neurologische Universitätsklinik, Hansastraße 9, D-7800 Freiburg, F.R.G. and [2]Department of Psychology C-009, University of California at San Diego, La Jolla, CA 92093, U.S.A.

(*Received* 5 *October* 1988; *in revised form* 15 *March* 1989)

Abstract—Rod vision has a duality of organization: at mesopic luminances rod signals have access to a slow, sensitive pathway (which we refer to, following Stiles, as π_0) and a fast, insensitive pathway (π_0'). The phase lag between the two rod signals increases with frequency until at 15-Hz the rod signals transmitted through the two pathways emerge *out-of-phase*, so that destructive interference produces a nulling of the apparent flicker. Relative to the cones, the phase lag of π_0' is roughly half that of π_0. Thus at 15-Hz π_0' signals can be out-of-phase with cone signals, so that the signals from the slower pathway, π_0, are actually *in phase* with cone signals. We have investigated the frequency response, adaptation behavior and phase characteristics of the two rod processes. The slower process, π_0 is more sensitive than π_0', and dominates from absolute threshold up to low mesopic levels. The adaptation of π_0 seems not to be associated with a change in time constant, but rather with simple response compression or sensitivity scaling. The time constant of π_0', however, does change with adaptation. There are large differences in the way that light adaptation changes the sensitivity of the two processes: signals from π_0' may evade part of the postreceptoral sensitivity regulating mechanism normally associated with rod vision. The ability of signals from π_0 and π_0' to reinforce or cancel each other, however, suggests that they are later reunited in a common pathway.

Flicker Modulation sensitivity Phase differences Rods Rod–cone interactions

INTRODUCTION

One of the primary manifestations of rod–cone duplicity in human vision is that the speed of processing of rod or scotopic vision is considerably slower than that of cone or photopic vision. This was demonstrated by Ives (1922) who determined the transitional or critical flicker frequency (c.f.f.) that marks the disappearance of perceived flicker with increasing stimulus frequency. He found that c.f.f. remained low and relatively constant for light intensities in the high scotopic or low mesopic range. However, as soon as the light intensity was sufficient to bring cones into play, the c.f.f. began to increase, ultimately rising far above the scotopic limiting value.

This double-branched c.f.f. vs log intensity curve, along with the double-branched dark adaptation curve (Kohlrausch, 1922), the double-branched visual acuity vs intensity curve (Shlaer, 1937) and the double-branched threshold vs intensity (t.v.i.) curve (Stiles & Crawford, 1934), has long been one of the cornerstones of the duplicity theory of vision (von Kries, 1894). Recently, however, the theoretical picture, which divides visual function into rod and cone branches, has been complicated by evidence that the human rod system itself has an internal duality. The duality is revealed in c.f.f. vs log intensity curves and in t.v.i. curves that have two distinct branches, even though rod vision alone is involved in detection (Conner & MacLeod, 1977; Conner, 1982). It now appears that the familiar, sluggish rod process that operates at very low light levels (referred to by Stiles as π_0) is accompanied by a faster but less sensitive rod process that comes into play at higher light levels (referred to here as π_0', in rough analogy with the modified high-intensity states of the cone mechanisms identified by Stiles, 1959). In this paper we investigate psychophysically (i) the phase and amplitude characteristics of the π_0 and π_0' signals at different light levels, and (ii) the way in which the π_0 and π_0' signals interact with one another and with signals from the cones. The results demonstrate striking differences between π_0 and π_0' in their phase lags (which can be about 360° and 180° respectively relative to a cone

---

*To whom correspondence should be addressed.

reference at 15 Hz) and also in the way that their sensitivity is regulated by light.

GENERAL METHODS

Subjects

The three authors served as the observers during these experiments. LTS and AS have normal colour vision. DIAM is deuteranomalous. LTS is slightly myopic (−2D), DIAM is slightly hypermetropic (+1D) and AS is emmetropic. Corrective lenses were not necessary for LTS or DIAM in these experiments.

Stimuli

In the experiments described below, one, two or three spatially coextensive test lights were used. They subtended 6.2° of visual angle in diameter and were centred 13° temporally from the observer's fovea in his right eye. In general, one or two green lights (500 nm) served as the rod stimuli and a single red light (either 668 or 680 nm) served as the cone reference stimulus. The wavelength characteristics of the test stimuli were shaped by interference filters, having half amplitude bandpasses between 7 and 11 nm. The intensities of the stimuli were modulated over time to give square-wave flicker, which could be varied in frequency and temporal phase. The observer's fixation was aided by a tiny orange-red lamp.

During many of the experiments, the test lights were superimposed on a concentric deep-red steady background, subtending 11.5° of visual angle. The colour of this field was selected by a gelatin cut-off filter (Kodak Wratten No. 70), and heat-absorbing glass. Measured *in situ* these filters transmitted less than 0.03% of maximum below 600 nm, and 50% at 660 nm with peak transmission at about 684 nm. This long-wavelength field was chosen to reduce as much as possible the sensitivities of the long (LWS)- and middle (MWS)-wavelength sensitive cones, relative to that of the rods. By selecting rod test stimuli with a wavelength of 500 nm, close to the peak of the scotopic visual sensitivity function, and presenting them on various intensities of deep-red background field, we could investigate the dependence of rod temporal sensitivity on adaptation level up to quite high scotopic levels (as, for example, in the flicker-threshold vs intensity or f.t.v.i. curves of Fig. 1).

For the cone reference stimulus, obtaining good isolation at low temporal frequencies and low scotopic adaptation levels was more

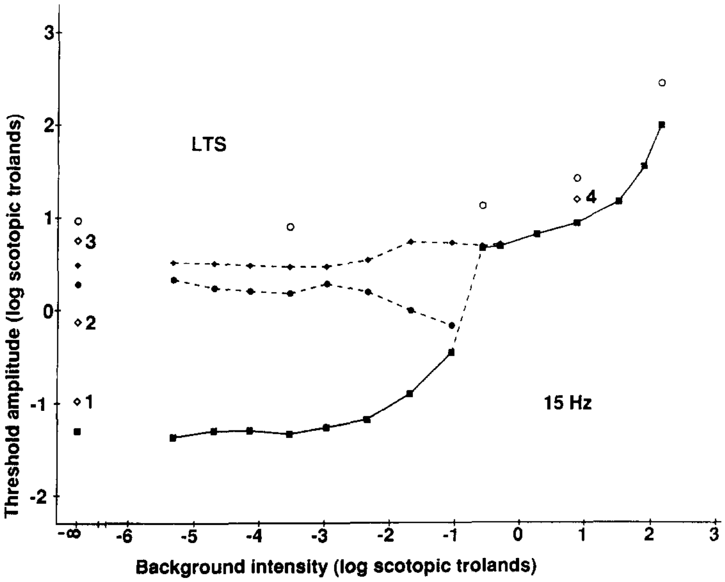

Fig. 1. 15 Hz flicker detectability data for LTS. The squares represent a conventional *flicker threshold vs intensity* function, i.e. they represent the lowest amplitude at which flicker can just be seen measured as a function of intensity. The broken line delimits a nulled region within which flicker cannot be seen. Data points designating the lower and upper limits of this nulled region are indicated by filled circles and diamonds, respectively. The open circles are cone thresholds measured during the cone phase of recovery following a 7.7 log photopic td-sec bleach. The open diamonds numbered 1–4 refer to intensity levels at which the modulation sensitivities and phase lags were measured (see Fig. 6). According to our model, significant sections of many of our experimental curves reflect the joint activity of π_0 and π_0'. We have therefore avoided labelling sections of our curves "π_0" and "π_0'".

difficult. This is because, in the fully dark-adapted eye, the absolute sensitivity of the peripheral rods to low temporal frequencies is greater than or comparable to that of the cones at almost all wavelengths (Wald, 1945). Distortions of phase lag data collected at our lowest scotopic adaptation level confirmed that rods were indeed detecting 668 or 680 nm test lights. On LTS we made extensive tests and checks to ensure that cone isolation was achieved. In some experiments, to avoid rod detection of the cone reference flicker we used a "silent exchange" test stimulus in which the red (680 nm) cone stimulus was combined with a coextensive green (530 nm) test stimulus, flickering in counterphase with it. The time-average scotopic illuminances of the red and green components were equated, leaving the photopic illuminance of the red component about 200 times greater than that of the green component. Thus the alternating red and green (680 and 530 nm) stimuli presented the cones with flicker, but the rods with a relatively dim and steady stimulus. In most experiments, we could avoid such complicated controls by simply increasing the amplitude of the 680 nm reference light. Increasing the amplitude apparently increased the cone signal much faster than the rod signal, so that the former soon swamped the latter (see also MacLeod, 1974).

Apparatus

A four channel Maxwellian view stimulator (see also Stockman, MacLeod & DePriest, 1989) produced the flickering rod and cone test stimuli as well as the steady background field. All four channels originated from a 1000 W Xenon arc lamp, run at constant current. Channels 1 and 2 combined to produce the rod test stimulus, with Channel 1 providing the steady component of the modulated 500 nm light and Channel 2 the flickering component. To maintain a constant time-averaged intensity, while varying the modulation, adjustable polarizers in these two channels were antagonistically yoked, so that increasing the steady component reduced the flickering component, and vice versa. Channel 3 usually provided the deep red background field, but at low scotopic adaptation levels in some control experiments for LTS it provided the 530 nm light that cancelled the rod component of the 680 nm cone reference stimulus. Channel 4 provided the 668 or 680 nm cone reference stimulus.

Circular aperture stops, placed at the focal points of the Xenon arc in each channel, restricted the images of the arc to less than 2 mm in diameter at the plane of the observer's pupil. Circular field stops placed in collimated beams in each channel defined the test and adapting fields as seen by the observer. Shutters (Vincent Associates, Model No. 26L) were positioned in each channel near focal points of the Xenon arc. These shutters have rise and fall times of 0.6 and 0.9 msec, respectively, and are rated for frequencies up to 100 Hz. Each was run independently by separate shutter drivers connected to frequency generators (Wavetek). With this arrangement we could obtain reliable square-waves up to the highest frequencies that we required (20 Hz for AS and LTS, 25 Hz for DIAM). The optical waveforms so produced were monitored periodically using a Pin-10 photodiode (United Detector Technology) and oscilloscope. Fine control over the luminance of the stimuli was achieved by variable, circular neutral density wedges (Kodak, Inconel), positioned close to image points of the Xenon arc, and by the insertion of fixed neutral density filters in parallel portions of the beams.

The radiant fluxes of the various test and adapting field stimuli were measured at the plane of the observer's entrance pupil with a calibrated EG&G Radiometer/Photometer.

Experiment I. Rod Flicker Thresholds and Flicker Nulls as a Function of Scotopic Intensity

Introduction

A duality in rod vision is suggested by clear breaks in rod critical flicker frequency data (Conner & MacLeod, 1977; Hess & Nordby, 1986) and rod flicker threshold data (Conner, 1982), measured as a function of background intensity. In the curve relating rod c.f.f. to the logarithm of scotopic luminance, for example, one branch rises until it reaches an asymptote (generally around 15 Hz) above 0.03 scotopic troland (scot. td; 1 scot. td = $10^{5.66}$ quanta/sec/deg^2 at 500 nm or approx. 4 isomerizations/sec/rod; see Wyszecki & Stiles, 1982, p. 103; Baylor, Nunn & Schnapf, 1984). Then near 1 scot. td there is an abrupt change of slope and a second branch emerges extending to frequencies as high as 28 Hz. Similarly, in rod flicker-threshold-vs-intensity (f.t.v.i.) curves, there are discontinuities in the flicker detection threshold behaviour that occur between low and high mesopic levels, with the prominence of the discontinuity depending upon flicker frequency. The branch following the discontinuity has generally been overlooked partly because it is only clearly seen when special procedures (e.g. Stiles, 1939) are adopted to ensure that it is unobscured by cone responses (Conner & MacLeod, 1977) or when individuals deficient in cone vision are used as observers (see, for example, Hess & Nordby, 1986). It is also possible that on occasions the second branch has been overlooked, simply by being misidentified as a cone branch.

In the first experiment, we measure flicker sensitivity at 8 and 15 Hz, choosing test and background conditions to favour rod detection. We find that the flicker curve is distinctly double-branched at 15 Hz, but not at 8 Hz. Moreover, the flicker curve at 15 Hz is more complex than has previously been reported (Conner, 1982), since there is a region where "self-cancellation" or "self-nulling" of the 15 Hz signal occurs. By self-cancellation or self-nulling we mean that a single flickering light appears steady or nulled, even though flicker reappears at higher *and* lower flicker amplitudes. (This type of null should not be confused with a conventional flicker null, in which two flickering lights must be used for cancellation to occur.) Self-cancellation was first demonstrated for mesopic stimuli that are detected by rods *and* cones by MacLeod (1972, 1974), and later confirmed by van den Berg and Spekreijse (1977). MacLeod explained his result by invoking large phase differences between rod and cone signals, the rods being more sluggish than the cones (Arden & Weale, 1954; Gouras & Gunkel, 1964; Gouras & Link, 1966; Veringa & Roelofs, 1966; Kelly, 1972). Presumably the signals from the two systems interfere destructively, subjectively cancelling each other when they differ in phase by 180° and are similar in magnitude. MacLeod (1972) found that cancellation between the rod and cone signals occurred best around 7.5 Hz. At this frequency, a single mesopic flickering stimulus gave rise to a null, even though flicker could be clearly seen at higher (photopic) and lower (scotopic) luminances, or during the cone plateau following a bleach. This phenomenon he labelled the mesopic flicker null. (For our stimulus conditions, we do not find a mesopic null in the region of 7.5 Hz; we will explain why below.)

This mesopic null at 7.5 Hz is consistent with standard notions of visual duplicity and with the unitary character of the rod mechanism. The scotopic null we now report at 15 Hz, however, is not; since it occurs at intensities below the cone threshold, it suggests the operation of *two* rod processes, generating opposite phase signals in response to the same stimulus.

Procedure

The observer dark adapted for at least 40 min, prior to an experimental session. He then adjusted the intensity of the square-wave flickering rod stimulus until flicker was just detectable in the presence of a background light of fixed intensity. The observer repeated the threshold setting several times, alternately beginning at a test intensity above or below the previous setting. Every threshold reported here is the mean of at least four independent settings, which rarely spanned a range exceeding 0.1 log unit of intensity.

After completing flicker threshold settings at several background intensities, the observer determined, in a separate experiment, the limits of the null region. He increased the intensity of the suprathreshold rod stimulus until the sensation of flicker vanished. (This was generally possible for 15 Hz but not for 8 Hz.) This setting, repeated several times, defined the lower limit of the null region. The upper limit of the null region (i.e. the intensity level of the suprathreshold rod stimulus at which the sensation of flicker is once again seen) was similarly defined.

Two complete sets of data were obtained for LTS and AS in two separate sessions. DIAM completed only one session.

Results and discussion

Figures 1, 2 and 3 show average thresholds measured for 500 nm light at 15 Hz for the observers LTS, AS and DIAM. In the figures, the scale of the abscissae indicates the intensity of the red background field in log scotopic td; the scale of the ordinate indicates the amplitude of the rod (500 nm) flickering test stimulus. The first thing to note is that the t.v.i. function of each observer (squares) contains two distinct branches. They intersect at about 0.25 log scot. td (total time-average intensity), a value very close to that found by Conner (1982) for similar observation conditions (see his Fig. 10). The lower branch has been previously identified as the low intensity rod mechanism (which we are calling π_0); the higher branch, as the high intensity mechanism (which we are calling π_0'). We know that this second branch is not a cone

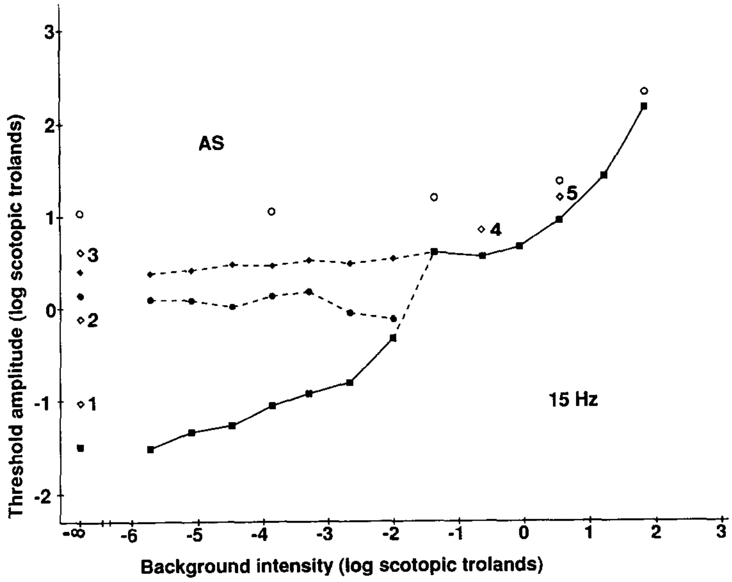

Fig. 2. 15 Hz flicker detectability data for AS. Details as for Fig. 1. The open diamonds numbered 1–5 refer to intensity levels at which the modulation sensitivities and phase lags were measured (see Figs 5 and 7).

branch on several grounds (for which, see Conner, 1982), but in the first instance because the cone flicker thresholds lie above it. This is shown by the open circles, which mark the thresholds of the middle-wavelength sensitive (MWS) cones. These were measured during the plateau that terminates the cone phase of recovery from a white bleaching light of about 7.7 log photopic td-sec. For the deuteranomalous observer DIAM, the separation between the rod and cone flicker thresholds is larger, being at least 1.0 log unit. This is not unexpected because the spectral sensitivity of his MWS cones is shifted towards long wavelengths. Such a shift affords better rod and cone isolation in two ways: first, his MWS cones are slightly less sensitive than normal to the 500 nm test stimulus and, consequently, less likely to detect it; second, his MWS cones are more sensitive than normal to the deep-red background stimulus

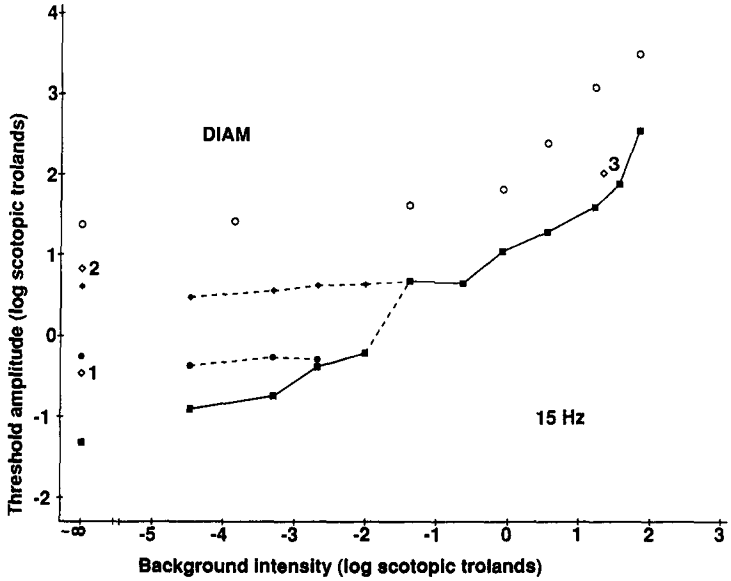

Fig. 3. 15 Hz flicker detectability data for DIAM. Details as for Fig. 1. The differences between the 15 Hz data for DIAM and those for AS and LTS are largely a result of DIAM's deuteranomaly (see text). The open diamonds numbered 1–3 refer to intensity levels at which rod–cone phase lags were measured (see Fig. 8).

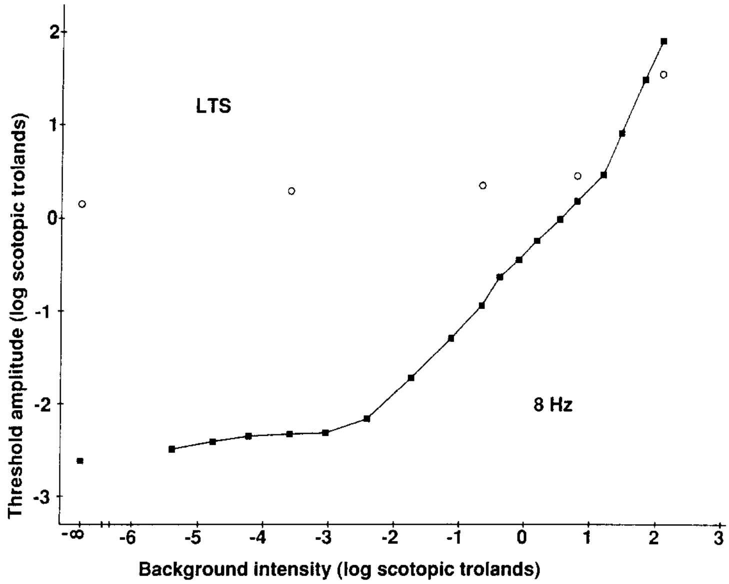

Fig. 4. 8 Hz flicker detectability data for LTS. The filled squares represent a *flicker threshold vs intensity* function. The open circles are cone thresholds measured during the cone phase of recovery following a 7.7 log phot. td-sec bleach. No nulled region was found under these conditions.

and, consequently, more strongly adapted by it.

For all subjects the two branches were separated by a range of luminance within which the flicker was completely invisible. The lower and upper limits of this nulled region are denoted by filled circles and diamonds respectively. Flicker could be seen at dimmer or brighter intensities, but it quickly vanished whenever the flickering field's intensity was set within the area demarcated by the broken lines. We assume that within this null region both processes are active, but that their signals interfere destructively to cancel the perception of flicker.

In each flicker threshold curve, the upper branch (upper continuous curve) lines up roughly with the upper limit of the no flicker region (upper dashed curve). Although this region appears to end abruptly with the emergence of the upper branch, it probably extends somewhat *beneath* the upper branch of the threshold curve at higher intensities. That there is no lower boundary corresponding to this extension of the nulled region is probably because at higher adaptation levels the π_0 signal is dominated by the π_0' signal, so that the π_0 signal alone never exceeds threshold.

The roughly parallel course of the π_0' curves and the cone plateau thresholds in Figs 1–3 might suggest that π_0' thresholds are controlled mainly by a photopic adaptation mechanism. This, however, is not the case: measurements (not shown) using shorter wavelength background light (450 nm, 500 nm, 520 nm and 560 nm), as well as long-wavelength background light showed a roughly scotopic sensitivity to the background field for both π_0 and π_0'. (Of course, this does not rule out the possibility that small cone effects may exist at long background wavelengths.)

Figure 4 shows flicker thresholds for observer LTS measured at 8 Hz. Here a transition between the two rod processes is not so readily apparent. Nevertheless, there is a suggestion of an inflection near the same background intensity as the abrupt change in slope in Fig. 1. This inflection has since been observed in the typical, complete achromat and in other normal observers (Stockman, Sharpe, Fach & Nordby, 1989).

The final, steeply rising segment of the 8 Hz curve, emerging near 2 log scot. td, undoubtedly corresponds to the saturation of the rod mechanism and is similar to what has been measured before in normal observers using flashed test stimuli and with special procedures to eliminate cone intrusion (Stiles, 1939; Aguilar & Stiles, 1954).

For 8 Hz flicker, increasing the intensity of the flickering rod (500 nm) stimulus above its threshold did not result in any scotopic (i.e. $\pi_0 - \pi_0'$) null or any apparent reduction in flicker amplitude. Evidently at this frequency, the two rod signals differ in phase by much less than the 180° needed for cancellation. For this frequency, cancellation can occur only between the slow (π_0) rod signal and the cone signal

(MacLeod, 1972; and our Figs 6 and 7, below). We fail to observe a mesopic null, however, presumably because of the intrusion of the π_0' rod process, which has a phase lag intermediate between that of π_0 and the cones (see below).

Although our findings are otherwise consistent with those of Conner (1982), they contradict his statement that a null is not detected when the flickering stimulus is spatially uniform. As with the rod–cone null, the rod–rod ($\pi_0 - \pi_0'$) null depends more critically on the frequency and luminance of the stimulus, than on its spatial homogeneity. It is possible (as discussed below) that Conner's counterphase-modulated bipartite field was useful in suppressing flicker signals generated by light scattered within the eye. But one of us (DIAM), who also served as an observer in some of Conner's experiments, had no difficulty, then or now, in observing a scotopic null when a spatially homogeneous test field was used.

Experiment II. Rod Modulation Sensitivity

Introduction

Our interpretation of Expt I is that there are two rod pathways, π_0 and π_0', with markedly different dynamics and adaptation behaviour. To explore this further, we measured the frequency responses of the rods at a number of intensity levels. Two of these levels were chosen to straddle the nulled region found at 15 Hz; according to our interpretation of the data from Expt I, we expect the frequency response functions at these levels to reflect the mixed properties of both π_0 and π_0' (see below). Two other levels were chosen at quite low and quite high scotopic luminances; at these levels we expect π_0 and π_0', respectively, to dominate the frequency response functions. The particular intensity levels at which temporal modulation sensitivities were measured are indicated by the diamond shaped symbols numbered 1–4 in Fig. 1 for LTS, and 1–5 in Fig. 2 for AS. Phase lag measurements for both AS and LTS measured at these same levels are shown in the next section (see Expt III). The luminance of the deep red background in photopic td can be approximated by multiplying the luminance given in scotopic td by 100.

Procedure

In order to measure the frequency response of the rods, we needed to vary modulation depth, while keeping the time-average intensity of the stimuli constant. We achieved this by means of two linear polarizers placed in Channels 1 and 2 and antagonistically yoked together. The test and background intensities were set at one of the numbered levels shown in Figs 1 and 2. Then, for several square-wave flicker frequencies, 2, 5, 7, 10, 15, 17.5 and 20 Hz, the observer's sensitivity was determined by finding the smallest modulation that could be distinguished from a steady light. The observer set each modulation threshold at least four times within each experimental session. The plotted modulation sensitivities are the averages of settings made during at least four separate experimental sessions.

Results and discussion

Figure 5 displays the average rod modulation sensitivities for observer AS. The modulation sensitivity functions, measured for LTS (not shown), are similar in shape. The squares are for the lowest intensity used (Fig. 2, no. 1; 0.048 scot. td), an intensity at which the sensitivities are expected to reflect the frequency response of π_0 with little or no influence from π_0'. At this level, the frequency response is

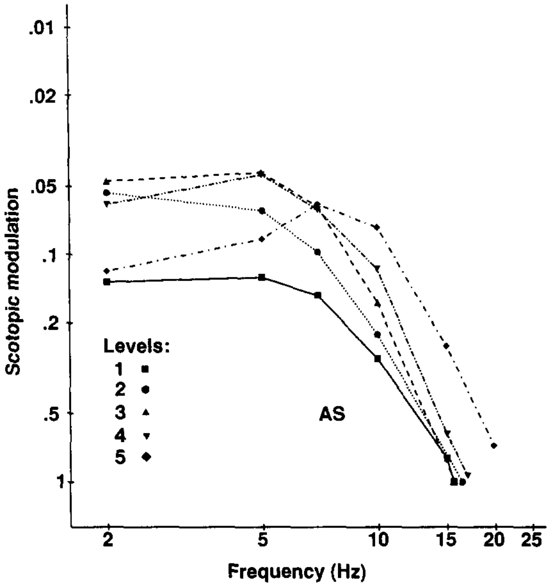

Fig. 5. Rod modulation sensitivity data for AS measured at five adaptation levels. The numbers correspond to those given in Fig. 2: (1) 0.048 (squares), (2) 0.38 (circles), (3) 2.04 (triangles), (4) 3.69 (inverted triangles) and (5) 11.15 (diamonds) scot. td. For the three lowest levels the 500 nm rod stimulus was presented without a background. For the two highest levels a deep red background was present. The contribution of the background to the scotopic intensities given above was 0.22 (inverted triangles) and 3.39 (diamonds) scot. td.

characteristic of a low pass filter: it has a plateau between 2 and 7 Hz, then drops quite sharply with increasing frequency reaching the c.f.f. between 17 and 20 Hz.

The diamonds correspond to the highest intensity used (Fig. 2; no. 5; 11.15 scot. td). At this intensity (which is well above the scotopic null) the sensitivities are expected to reflect the frequency response of π_0'. The function is markedly bandpass in shape (in spite of our use of square-wave flicker): it rises gradually to a peak between 5 and 10 Hz, and then falls off steeply with increasing frequency until reaching c.f.f. near about 20 Hz.

The modulation sensitivity functions measured at intensities between these two extremes might be expected to be intermediate in shape between the low-pass function (squares) and the band-pass function (diamonds). This simple prediction, however, is unlikely to be correct for a number of reasons. One reason, which was mentioned above, is that the modulation sensitivities measured at the intermediate intensity levels just below (circles, Fig. 2, no. 2; 0.38 scot. td) and just above (triangles, Fig. 2 no. 3; 2.04 scot. td) the 15 Hz nulled region will reflect the influence of both rod pathways. Since we believe the signals from π_0 and π_0' to be out of phase at frequencies in the region of 15 Hz, destructive interference should cause a loss of sensitivity in that region. Thus, although the functions measured below and above the nulled region may largely reflect the properties of the more sensitive process, i.e. π_0 and π_0', respectively, it is likely that the functions will be distorted by the influence of the less sensitive process. Of course, instead of the destructive interference expected in the region of 15 Hz, there may actually be facilitation between the two processes at other frequencies; see the rod–cone phase lag data, below. This, in fact, seems to be the case.

The curve indicated by the circles in Fig. 5 corresponds to the intensity just below the nulled region (Fig. 2, no. 2). This function is considerably steeper than the function measured at the lowest level (squares), a difference that is consistent with the predicted effects of destructive interference in the region of 15 Hz. The results of Conner (1982; his Fig. 7) show a similar trend. The curve indicated by the upright triangles corresponds to an intensity just above the nulled region (Fig. 2, no. 3). This function is similar to the function measured just below the null and similarly shows a steep fall-off, plausibly attributable to destructive interference, at high frequencies.

The curve indicated by the inverted triangles was measured at the next highest intensity level, also above the null (Fig. 2, no. 4; 3.69 scot. td). In scotopic trolands the level is only 0.26 log unit more intense than the next lowest level (upright triangles). The difference in *photopic* intensity is much greater, however, since in the former case a 21 phot. td deep red background has been added. This function does appear to be slightly more band-pass than the three functions measured at lower intensities, exhibiting a relative improvement in sensitivity between 5 and 10 Hz. However, when compared to the large difference in shape between this level (inverted triangles) and the next highest (diamonds), these differences are relatively small.

Experiment III. Rod–Cone Phase Lags

Introduction

The results of these experiments support two propositions: first, that there are two rod pathways (π_0 and π_0') and second, that the rod signals in these two pathways emerge in opposite phase at certain frequencies (e.g. at 15 Hz, but not at 8 Hz) so that when added together into a single resultant flicker signal they can interfere destructively to produce a steady signal (a scotopic flicker null). In order to explain why the null is restricted to a limited range of intensities, we must suppose that the relative strength of the π_0 and π_0' signals is dependent upon the intensity level. In other words, the light adaptation characteristics of the two processes must differ: at intensities below the null region, the amplitude of the flicker signal from the low intensity process π_0 supposedly exceeds that from the high intensity process π_0', and flicker is seen because the latter is insufficient to cancel the former when the two are added together; whereas at intensities above the null region it is the other way round.

This interpretation can be tested by measuring the phase lag of the rods relative to the cones as a function of frequency, both above and below the null intensity. The phase lag of the rod flicker signal should vary in a complex manner with stimulus intensity. For instance, if the frequency is such that the signals from the two rod processes are exactly out of phase, the resultant rod–cone phase lags should simply be the phase of whichever rod signal is of greater amplitude. There should accordingly be a 180°

phase discontinuity as the null intensity is crossed. If the frequency is such that the signals are not out of phase, the resultant rod–cone phase lags should vary smoothly between the phase differences of the two components.

Methods

The time-averaged intensity of the rod stimulus was set at one of the adapting levels used to measure the rod modulation sensitivities in Expt II (indicated by the numbered symbols 1–4 in Fig. 1, 1–5 in Fig. 2 and 1–3 in Fig. 3).

First, for each flicker frequency and condition of adaptation the observer was presented with a flickering 500 nm rod stimulus (the modulation of which was under his control), and a flickering 100% modulated 680 nm cone stimulus (the intensity, or absolute amplitude, of which was under his control). Before adjusting the relative phase of the two stimuli, the observer set each stimulus to just above the flicker threshold. (The flicker threshold for the 680 nm light was set in the presence of a steady 500 nm rod test light of the same time-average intensity as the *modulated* 500 nm light, and the modulation threshold for the 500 nm light was set in the presence of a steady 680 nm light of the same time-average intensity as the just supra-threshold, flickering 680 nm light.) At some higher frequencies, at which the rod modulation was close to or below threshold, the modulation of the 500 nm light was set to 100%.

The flickering rod and cone components were then superimposed, and the observer attempted to null the subjective flicker by adjusting their relative phase. Usually, the subject (i) made an approximate setting of the point of minimum flicker, then (ii) made fine adjustments of either the modulation of the rod stimulus or the amplitude of the cone stimulus in an attempt to improve the minimum, and lastly (iii) made the final phase settings. Often steps (i) and (ii) were repeated more than once. Four settings were recorded at each frequency. An additional facility available to the subject was a switch that inverted the relative phase of the rod and cone stimuli by 180°. At any point in his settings the subject was thus able to compare the phase at which the flicker appeared minimal to a phase opposite to it at which the flicker usually appeared maximal. This helped to ensure that the minimum flicker was not erroneously achieved by reducing the flickering stimuli below threshold. Our observers very quickly became skilled at making reliable phase settings, despite the apparent complexity of the task. Phase settings could sometimes be made even when one of the test lights was slightly below its conventionally-obtained modulation threshold (see General Discussion).

For each of the four intensity levels of the stimulus, the rod–cone phase lags were measured at several flicker frequencies between 2 and 20 Hz. The measurements were repeated between three and five times in separate experimental sessions and then averaged.

Results and discussion

Figures 6 (observer LTS) and 7 (observer AS) display the average rod–cone phase lags as a function of flicker frequency for the intensity levels indicated in Figs 1 and 2 and discussed above (Expt II, Introduction). For the two lowest levels (squares and circles), which are both below the scotopic null, the functions are approximately linear, the phase lag increasing rapidly with a slope of about 30° per Hz. If the phase lags are due to a simple delay between the responses of π_0 and the cones, then this slope implies that the π_0 signal lags behind the cone signal by about 80 msec. This is close to the value reported by MacLeod (1972, 1974) and

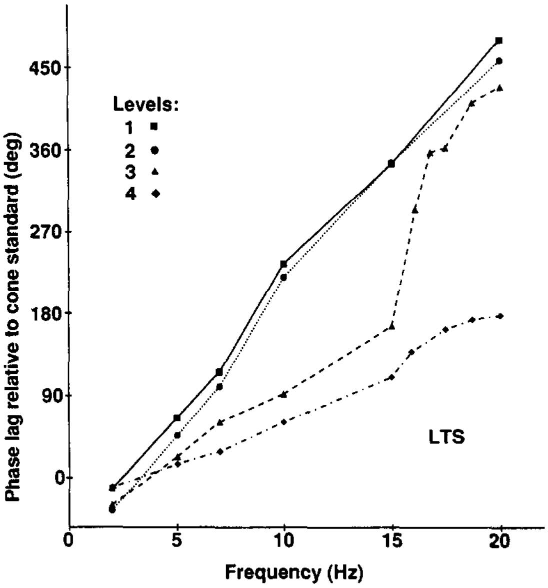

Fig. 6. Phase lag data for LTS measured at four adaptation levels. The numbers correspond to those given in Fig. 1: (1) 0.054 (squares); (2) 0.37 (circles); (3) 2.82 (triangles) and (4) 14.59 (diamonds) scot. td. For the three lowest levels the 500 nm rod stimulus was presented without a background. For the highest level a deep red background was present; the time averaged intensities of the test and background fields were 7.51 and 7.08 scot. td, respectively. All phase lags are measured relative to a cone standard.

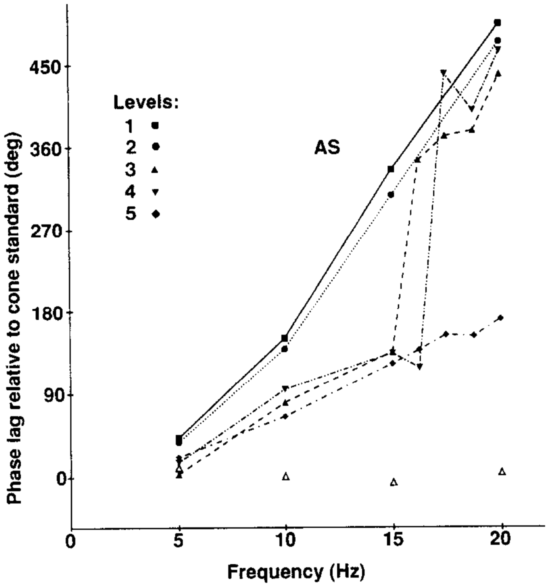

Fig. 7. Phase lag data for AS measured at five adaptation levels. The adaptation levels and their associated symbols are the same as for Fig. 5. Additional data obtained during the cone plateau following a 7.7 td-sec. bleach at the adaptation level of 2.04 scot. td are shown as open triangles. All phase lags are measured relative to a cone standard.

that (75 ± 10 msec) reported by van den Berg and Spekreijse (1977).

A consistent feature of the results for both subjects is that there is little or no change in phase lag between the two lowest intensity levels, despite a seven or eightfold increase in scotopic luminance. This similarity suggests that there is little change in the time constant of the rod response within this range, and that the same rod process, which we call π_0, is operating at both levels. The work of MacLeod (1972, 1974) was carried out at intensity levels that fall within this range, but his conditions differed in other ways (e.g. smaller field size). His results suggest a rod–cone phase lag of 180° in the region of 7.5 Hz. Our results place the frequency at which π_0 and the cone response are out of phase at a slightly higher value: approx. 8.5 Hz for DIAM (Fig. 8, squares); 9 Hz for LTS; and 11 Hz for AS. The response of π_0 lags behind that of the cones by a whole cycle at about 16 Hz for all three subjects.

At the highest level (diamonds), which is well above the scotopic null, the operative rod mechanism is π_0'. The functions of both observers are again approximately linear, but the slopes, between 10.5 and 11.5° per Hz, are considerably shallower than those at the lowest levels. If the phase lags were due to a simple delay between the responses of π_0' and the cones, then these slopes would suggest that the π_0' signal lags behind the cone signal by about 30 msec.

In comparing the results for the different intensity levels it should be remembered that the light adaptation of the cones changes considerably between levels. Since the rod phase lags must be measured *relative* to the cones, the measured π_0 and π_0' phase lags differ not only because of inherent differences between the two rod processes, but also because of differences in the speed of the cone response at the different intensity levels. Proper allowance for the light adaptation of the cones would, therefore, slightly reduce the intensity-dependence of the inferred rod phase lags shown in Figs 6 and 7.

At the adaptation level slightly above the scotopic null (triangles), and at the slightly higher level measured for AS only (inverted triangles, Fig. 7), the relationship between phase lag and test frequency is not linear. Rather the curve has two segments separated by a sharp discontinuity: the lower segment has a shallow slope, similar to that found for the highest intensity curve; whereas the upper segment has a steeper slope similar to that found for the lower intensity curves. To delineate this discontinuity more precisely we measured the phase lag at closely spaced intervals between 15 and 20 Hz. The abrupt jump occurs just above 15 Hz (triangles), or just above 16 Hz at the higher intensity level (AS, inverted triangles).

At 15 Hz, just before the discontinuity, the difference between the phase lags measured immediately above and immediately below the scotopic null is very close to 180°. For LTS the difference is 180°, and for AS 172°. These differences provide strong support for our hypothesis that the scotopic null is caused by destructive interference between two rod signals that are in opposite phase. Moreover, since there is nearly a full cycle phase difference between the rod signal just *below* the null and the signal from the cone standard (a phase difference of 307° for AS, and 346° for LTS), it is extremely unlikely that a cone signal can be responsible for the nulling of the low intensity rod signal.

The discontinuity above 15 Hz most likely represents a transition from the π_0' pathway to the π_0 pathway. At frequencies below 15 Hz, the phase lags are close to those determined at higher intensities for π_0', while above 17 Hz, they are close to those determined at lower intensities for π_0. But why should such a transition occur and why should it be so abrupt? If the two rod processes are indeed independent, then our results suggest that the sensitivity of π_0' must fall *more steeply* with frequency than that of π_0 in this frequency range. A rapid phase transition, such as the one that we observe, is possible provided that the two rod signals are close to out of phase (which, according to our results, they are). We suppose that with increasing frequency, the signals from both π_0 and π_0' decline, but the π_0' signal declines more rapidly with frequency than the π_0 signal. Thus, at frequencies below the discontinuity π_0' dominates, but above the discontinuity π_0 is more sensitive. There does seem to be some modest evidence that the high frequency slope of π_0' is steeper than that of π_0 in the modulation sensitivity data of AS (compare squares and circles with triangles and inverted triangles in Fig. 5). But it should be remembered that near 15 Hz the steepness of the modulation sensitivity functions can be influenced by destructive interference between the *two* processes as well as by the rate at which each loses sensitivity with increasing frequency.

Phase lags were also measured for AS, during the cone plateau of dark adaptation following a 7.7 td-sec white bleach, at an adaptation level normally just above the null (2.04 scot. td). Although the phase settings were comparatively difficult to make (since the 500 nm stimulus was below cone flicker threshold at higher frequencies), the data (open triangles, Fig. 7) are all consistently close to zero delay. The large non-zero phase delays found after complete dark adaptation, therefore, must reflect delays introduced by rod detection of the 500 nm test light. Cone contamination would have the effect of skewing our phase settings towards delays of 0° (or 360°).

Rod–cone phase lags were also obtained for DIAM. These data are shown in Fig. 8 for three intensity levels: (i) an intensity below the null (0.17 scot. td; squares); (ii) an intensity slightly above the null (3.47 scot. td; triangles and inverted triangles); and (iii) an intensity high above the null (72.18 scot. td total, which was composed of a 51.28 scot. td test light and a 20.89 scot. td deep-red background; diamonds). For two conditions (squares and inverted triangles), the Stiles–Crawford effect of the first kind (i.e. the marked directional sensitivity of the cones, but not the rods, to the pupillary angle of entry of light) was exploited to minimise cone intrusion in the response to the 500 nm stimulus. This was done by deflecting the beam carrying the test stimulus so that it entered the pupil at an eccentricity of 2 mm from the pupil centre, in a direction chosen to maximise cone sensitivity loss. This provided an extra 0.3 log unit or more of rod isolation. In addition, we achieved better rod isolation for DIAM than for either AS or LTS, simply because his MWS cones are less sensitive to the 500 nm test light (see Fig. 3). This improvement in isolation, together with peripheral pupillary entry of the rod test lights, makes it unlikely that the functions denoted by the squares and inverted triangles are significantly influenced by cones. In addition to the peripheral pupillary entry of the test lights, the test fields for these two conditions (squares and inverted triangles) were surrounded by an equiluminous annulus.

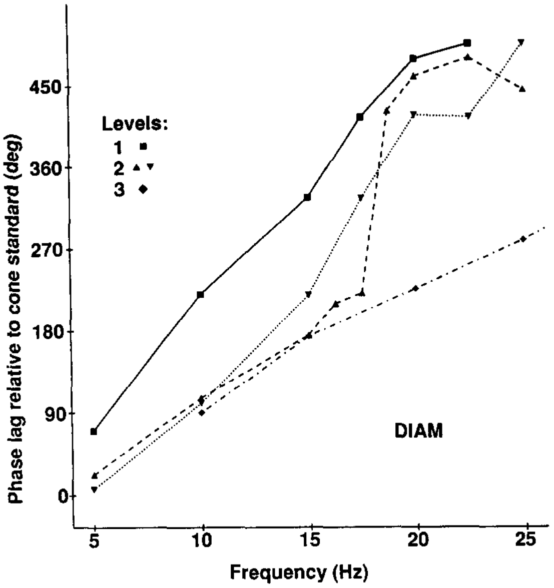

Fig. 8. Phase lag data for deuteranomalous observer DIAM measured at three adaptation levels. The numbers correspond to those given in Fig. 3: (1) 0.17 scot. td (squares); (2) 3.47 scot. td (triangles and inverted triangles); and (3) 72.18 scot. td (diamonds). For two conditions (squares and inverted triangles) the 500 nm rod stimulus was surrounded by a contiguous 500 nm annulus of the same time-averaged intensity; in addition, the stimuli entered the pupil at an eccentricity of 2 mm away from the pupillary centre to take advantage of the Stiles–Crawford effect (see text). For the two remaining conditions (filled triangles and diamonds) an annulus was not present and the stimuli entered the pupil at its centre. At the highest adaptation level a deep red background was present; the time average intensities of the test and background stimuli were 51.28 and 20.89 scot. td, respectively.

An equiluminous annulus was added to rule out an alternative explanation of the discontinuity found in the phase lag data for LTS and AS (triangles, Figs 6 and 7)—scattered or stray light. The alternative explanation rests upon the fact that at most levels the test lights are presented on a zero background. If the flicker signal from the region underlying the test light becomes very small with increasing temporal frequency (partly because the signals from the two processes null each other), then it is possible that the observer depends upon a weak flicker signal from the relatively unadapted regions around the edges of the test fields to make phase settings. This weak signal may result from scattered light, or perhaps from light falling directly on regions close to the edge of the test light, which because of eye movements are subject to a lower time-averaged light intensity than the regions closer to the centre of the test light. Since in both cases the light falls upon regions that are relatively unadapted, the low intensity or π_0 pathway should mediate detection of the flicker. Hence, as the signals from the centre are nulled and signals from the surround become prominent, the phase lag relative to the cones will flip from that of π_0' to that of π_0. Under this interpretation, the introduction of the surround should abolish the phase discontinuity.

The results for DIAM are similar to those for AS and LTS. As for the other observers, the phase lag measurements made for the stimulus intensity below the null (squares) are very different from those made for a stimulus intensity well above the null (diamonds). And, as for the other observers, the increase in phase lag with frequency appears to be linear for stimulus intensities both below and above the null, but the slope is much greater for the former than for the latter. Unlike for AS and LTS, however, both sets of measurements for DIAM can be followed up to 25 Hz because of the advantage of DIAM's deuteranomaly and (in the case of the lower level) the exploitation of the cone Stiles–Crawford effect. For the phase lag measurements made at a stimulus intensity just above the null, the flip from detection by π_0' to detection by π_0 is clearly evident, regardless of whether a surround is present or not (inverted triangles), and regardless of whether the pupillary entry is central (upright triangles) or peripheral (inverted triangles). This suggests that the π_0 pathway signals originating from the unadapted surround are not responsible for the flip, and that cones cannot be contributing importantly to it.

Experiment IV. Rod–Cone Phase Lags as a Function of Adaptation Level

Introduction

Our results discussed so far, in particular the phase lags of Expt III, support the proposition that there are two rod processes with markedly different phase characteristics. In the preceding experiment, the rod–cone phase lags measured as a function of frequency were obtained at a limited number of intensity levels. Those results indicated that the largest change in phase occurred between intensity levels straddling the 15 Hz nulled region, even at frequencies where π_0 and π_0' do not destructively interfere. In contrast, there was little change in phase between the two lowest intensity levels. To obtain more detailed information about phase change and about the transition from π_0 to π_0', we measured rod–cone phase lags as a function of intensity, using more closely spaced intensity levels, but fewer frequencies.

Procedure

The procedure was similar to that used in Expt III. Phase lags were measured as a function of adaptation level at frequencies of 8, 15 and 20 Hz for LTS, and 15 and 20 Hz for DIAM. The test stimulus was composed of a flickering 500 nm rod test light and a flickering 680 nm cone test light, the relative phase of which could be varied by the subject. The test lights were superimposed upon a steady deep red (Wratten no. 70) background light. As the overall scotopic intensity was increased, the ratio of the intensities of the rod test light and the deep-red background was held constant, thus keeping the scotopic modulation constant. The ratio of the intensities of the two lights was chosen so that the scotopic modulation was 69% for observer LTS and 77% for observer DIAM. The deep-red adapting light helped to reduce the possibility of the cones contaminating the response to the 500 nm rod test stimulus at higher test intensities. At very high intensities, however, the cones inevitably become more sensitive and dominate detection of 500 nm flicker. The amplitude of the 680 nm cone reference stimulus was kept close to cone threshold at all levels, and thus had little or no effect upon the rods, except at 8 Hz for the very lowest scotopic luminances (see Methods).

In one session, the observer made settings at each of an ascending series of intensity levels, increasing in steps of about 0.3 log unit. The scotopic intensity was increased by removing neutral density filters from a portion of the beam path common to the 500 nm test light and the deep-red background. Since these filters were not quite spectrally flat, we varied the position of a neutral density wedge in one of the beams to maintain a constant scotopic modulation.

The observer was required to adjust the relative phase of the rod and cone test stimuli to find the phase at which flicker was eliminated or minimized (it was generally possible to eliminate the perception of flicker to the satisfaction of the subject). Three or four phase settings were made at each intensity level. The phase lag data for LTS are averaged from settings obtained during two separate sessions. DIAM was able to complete only one session.

Results and discussion

Figure 9 shows the rod–cone phase lags obtained for observer LTS as a function of intensity. The scotopic intensity was increased by increasing the intensity of both the rod test field and the deep-red background field. The rod modulation was 69%. For the 8 Hz curve, the phase lag is very constant at about 190° from − 1.7 to nearly 0.0 log scot. td. That the phase lag should remain constant over a range of more than one and a half log units of intensity suggests that light adaptation does not alter the timing of the π_0 signal. This is consistent with the phase lags measured as a function of frequency in Figs 6–8. Above 1 scot. td, however, the phase lag falls quite rapidly, decreasing by 77° over 0.66 log unit (implying a maximum gradient in excess of 117° per log unit). This rapid decrease occurs in the same intensity range as the 15 Hz null, and may therefore reflect the transition from π_0 to the π_0' at 8 Hz. Beyond the transition there is a shallower decline in phase lag. This shallow decline probably reflects: (1) a speeding up of the π_0' signal above the transitional intensity range of 1–4 scot. td; and (2) the inception of cone intrusion in the response to the 500 nm test stimulus at still higher levels. At the highest adaptation intensities, the phase lag between the "rod" and "cone" stimuli is almost zero, indicating that there is no appreciable phase lag between the signals being produced by the two stimuli.

At 15 Hz the phase lag stays constant at about 370° for adapting levels between 0.05 and 1 scot. td (the same range for which the 8 Hz phase remained constant). Then it declines rapidly, between adapting intensities from 1 to 4 scot. td, to 180°. This is consistent with the transition of detection from the π_0 to the π_0' process. The phase lag remains constant at 180° for the next 1.0 log unit. Thereafter it starts to fall steeply to a value of 0° as the rod stimulus is increasingly effective on the cones. This zero

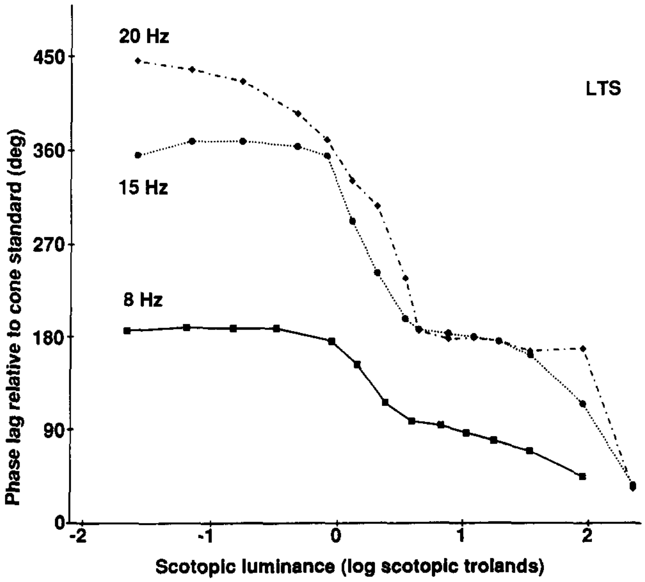

Fig. 9. Phase lag data for LTS measured as a function of scotopic luminance at flicker frequencies of 8 Hz (squares), 15 Hz (circles) and 20 Hz (diamonds). In all cases a 500 nm rod test stimulus was presented in the centre of a deep red background. The scotopic luminance was increased by increasing the intensity of both the test and background lights in tandem so that the scotopic modulation remained constant at 69%. The phase lags are measured relative to a cone standard.

phase lag at the highest intensity suggests that detection of the rod stimulus has completely passed to the cone mechanism so that both stimuli are being detected by the same class of photoreceptor.

The 20 Hz curve is quite similar to the 15 Hz curve at middle and high scotopic luminances, except for showing some gradual fall in phase delay in the π_0 range from 450° at 0.05 scot. td to 370° at 1 scot td. Since the more rapid change in phase occurs at a similar scotopic luminance at all three frequencies, the switch-over from the π_0 to π_0' pathway appears to be adaptation dependent and not strongly frequency dependent. The results for DIAM at 15 and 20 Hz, which are not shown here, are consistent with those for LTS.

BIPARTITE FLICKERING FIELDS

A display permitting a side-by-side comparison proved useful for demonstrating the large phase difference between 15 Hz signals above and below the self-nulling region. We set the amplitude of the 500 nm test field to double its amplitude in the middle of the nulled region (roughly 0.75 log scot. td for LTS). We then covered one half of the field (at the field stop) with a 0.6 log unit neutral density filter. With this arrangement weak flicker was seen in both halves of the field. According to our model the flicker on the dimmer side (which is just below the null intensity) should be seen more strongly by π_0 and that on the brighter side (which is just above the null intensity) should be seen more strongly by π_0', *and* there should be a phase difference of 180° between the flicker seen on the two sides. We were able to confirm this by adding a flickering cone light that could be flipped 180° in phase relative to the rod flicker. As expected, we found that flicker was seen strongly on the dim side, but was greatly reduced on the bright side, when the cone stimulus was added in similar phase. But when the cone stimulus was added 180° out of phase the reverse was the case.

With this bipartite field we were able to compare the effects of experimental manipulations upon the subjective salience of π_0 dominated flicker, on one side of the bipartite field, and of π_0' flicker, on the other side. We hoped that some manipulation might favour one of the two processes, and so provide us with more information about the underlying differences between the two processes.

Since π_0 and π_0' differ so radically in their temporal properties, we assumed it likely that they would also differ in their spatial organization. Such a difference is made plausible by the fact that in the low π_0 intensity range, the quantum flux is so small that flicker can only be monitored reliably by pooling the signals from many rods, whereas in the high π_0' range signals from individual rods could (in principle) preserve the flicker waveform. To manipulate the spatial characteristics of the stimuli, we introduced gratings (of 3.50, 2.33, 1.06 or 5.06 cycles per degree (cpd)) at right angles to the border of the bipartite field and modulated alternate bars in opposite phase. If π_0 and π_0' differ in the extent to which rod signals are pooled, some gratings will be better resolvable by one than by the other process, and will upset the equality between their signals, making flicker apparent where (in the absence of the grating) there had been a null. A change of intensity might then reinstate the null. The results did not support this prediction. Instead, at the three highest spatial frequencies we found that the nulling region actually extended to well above and well below the uniform-field null range (suggesting that at these spatial frequencies opposite phase flicker signals from alternate bars were cancelling each other within π_0 and π_0'). At 0.56 cpd there was a hint of flicker in the regions normally just below and above the null, but still less than in the case of the uniform field. The fact that the center of the null did not depend on the spatial structure of the stimulus suggests that neural excitation pools for the two processes are similar in size; the enlargement of the null at high spatial frequencies suggests that those pools are quite large, with diameters perhaps approaching 1° of visual angle. There is, however, already some evidence supporting a duality in spatial acuity within rod vision: Hallett (1962) found a clear change in the slope of the function relating acuity (measured by finding the minimum size of a dark disc that is detectable within a light surround) and scotopic luminance at 20° eccentricity from the fovea (but not at 7°). The break occurred at a background intensity near 0.5 log scot. td.

An attractive explanation of the adaptational and temporal differences between π_0 and π_0' signals is that the latter bypass part of the sensitivity regulating mechanism normally associated with rod vision, because they travel in pathways intended for cones. If π_0' shares a common pathway with cone signals, distinct from π_0, then it is possible (although not necessary) that cone masking stimuli may differentially suppress π_0' signals. In the bipartite field comparison, this differential suppression might be seen as an increase of flicker on the dim side and a decrease of flicker on the bright side. To test this we superimposed a variety of cone masks over the whole bipartite field and observed the change in the salience of the flicker on the two sides. The masks that we used were chosen to stimulate either short-wave cones or long-wave cones. The masks were either uniform fields, flickered rapidly (up to 35 Hz) or slowly (down to 2 Hz), or else gratings exposed steadily or flickered at 0.4 Hz or 2 Hz. In general, the results were suggestive of a slight selective suppression of π_0' flicker by cone masks, but our informal results were not striking, and were not completely consistent. The slight suppression is consistent with our field sensitivity measurements (see above), which indicate that the effects of cone stimulation on π_0' must be comparatively small, otherwise the field sensitivity of π_0' would not be rod dominated.

GENERAL DISCUSSION

Our results agree with earlier findings that the scotopic or rod visual system has an internal duality of organization. Duality has been previously suggested in the double-branched flicker responses of individuals with normal scotopic vision (Conner & MacLeod, 1977; Conner, 1982). In typical complete (rod-dominated) achromats many well-documented phenomena can be ascribed either to similar scotopic duality or else residual cone function: two branched increment thresholds (Hecht et al., 1948; Alpern, Falls & Lee, 1960; Blakemore & Rushton, 1965), dark adaptation (Lewis & Mandelbaum, 1943; Walls & Heath, 1954; Sloan, 1954, 1958; Alpern et al., 1960; Blakemore & Rushton, 1965) and temporal acuity (Hecht et al., 1948; Alpern et al., 1960; Blakemore & Rushton, 1965; Gouras & Gunkel, 1964). The former alternative best explains the two-branched temporal resolution function and is supported by the recent observations of Hess & Nordby (1986) and Sharpe & Nordby (1990).

The results presented here strongly suggest: (i) that there is a sluggish sensitive process, π_0, and a fast, less sensitive process π_0'; (ii) that the two processes differ in frequency response (especially in their phase characteristics) and adaptation behaviour; and (iii) that the signals from the two processes do not remain separate but may interfere destructively with each other and with cones over a wide range of frequencies and luminances. In short, the characteristics of π_0 and π_0' are qualitatively what is to be expected from two independent scotopic processes, which jointly participate in setting sensitivity under conditions where both are active and which jointly contribute to a resultant signal in some later common pathway where subjective flicker is encoded.

Relationship to other psychophysical work

The results of our 8 Hz flicker sensitivity measurements differ in interesting respects from comparable measurements made at 7.5 Hz by MacLeod (1972). MacLeod reported that, on increasing the amplitude of 7.5 Hz flicker, a nulled region is encountered well above absolute threshold (similar to the region that we report at 15 Hz, but causally different). Unlike him, we find no evidence of a mesopic null at 8 Hz (see Fig. 4). However, there is no inconsistency between the two results: the differences are rooted in the choice of test wavelength (and to a lesser extent in the choice of background wavelength). Because MacLeod used a yellow flickering test light, cones begin to detect the flicker *before* π_0'. Thus the rod–cone interaction that he found is between π_0 and the cones, which, since they are 180° out of phase at 7.5 Hz (see Figs 6–8), destructively interfere. We, however, used a 500 nm flickering test light, to which (relative to the yellow test light) the rods are more sensitive and the cones less sensitive. When the intensity of this light is increased, π_0' detects the flicker before the cones. Since the phase lag between π_0' and the cones is only about 90° at 8 Hz, these two signals cannot cancel and a "mesopic" null is not found. To observe the mesopic null in the region of 7.5 Hz requires, therefore, that conditions are chosen that *do not* maximally isolate the rods.

We note that both Conner and MacLeod are deuteranomalous. Although this point was not deemed important enough to mention in Conner and MacLeod (1977) or Conner (1982), the spectral sensitivity shift of the deuteranomalous trichromat's MWS cones allows rod isolation to be maintained to higher adaptation levels and flicker frequencies than is possible using normal subjects. The advantage in using deuteranomalous subjects can be seen at once on comparing the extent of rod isolation for LTS and DIAM at 15 Hz (see Figs 1 and 3).

The modulation sensitivities reported by Conner (1982; Fig. 7, page 147), roughly agree with our measurements, except that his functions tend to be slightly more band-pass at higher scotopic adaptation levels. Such a difference is to be expected, partly because we used square-wave flicker. But, although Conner did use sinusoidal modulation, his "modulation sensitivities" were actually derived from conventional flicker threshold measurements, in which the steady component of his stimulus differed from the flickering component in both area and colour. Specifically, his modulation sensitivities (and c.f.f.'s) were calculated from simple flicker threshold-vs-intensity threshold measurements obtained using a 519 nm, 9° diameter, flickering test light presented in the centre of a red, 13° background. As a result, modulation in his experiments is effectively "varied" by exchanging a flickering 519 nm, 9° field, with a red, 13° field. Although the time-average *scotopic luminance* is kept constant for a particular modulation sensitivity curve, the *photopic luminance* varies enormously, bearing an inverse relationship to the scotopic modulation. If cones do influence the sensitivity of either π_0 or π_0' these large imbalances in photopic luminance will distort the shapes of rod modulation sensitivity curves. (The definition of modulation given in Conner (1982; equation 1, p. 141) is wrong, though his data are correct. The definition underestimates modulation thresholds at low modulations.)

An obvious difference between our results and those reported by Conner (1982) is that each of our three subjects encountered a large region in which a *single* 15 Hz flickering test light appeared steady, caused (we argue) by destructive interference between the π_0 and π_0' signals. Conner, on the other hand, reported that "a null was never detected when the stimulus was uniform" (1982; p. 150). To obtain a null at 15 Hz Conner flickered the two halves of his 9° test field 180° out of phase. With this arrangement he produced a 15 Hz threshold function similar to those we obtained with a single field. From the work of Conner, then, we are left with the idea of two rod mechanisms that can destructively interfere, but to do so must act (in some unspecified way) over large distances of retina. In view of our informal observations that the spatial properties of π_0 and π_0' are quite similar, it is surprising that Conner was unable to obtain a null with a single field. One possibility is that there was a significant amount of scattered light (perhaps intraocular) in Conner's conditions. In the relatively unadapted regions of the retina surrounding the stimuli, detection of stray light flickering at 15 Hz will be dominated by π_0. Unlike flicker in the test fields, 15 Hz flicker in the surround will remain uncancelled, leaving, perhaps, a strong impression of flicker. By using two counterphase flickering half fields, Conner provided two temporally distinct sources of scattered light. Since the scattered light from the two sources was in opposite phase, destructive interference could have acted to reduce any impression of flicker in the surround, improving the overall subjective impression of a null.

Curves of c.f.f. vs log intensity usually show a dip where the rod and cone branches intersect, at a c.f.f. of about 15 Hz or slightly less (Brooke, 1951). This can hardly be explained by cancellation between π_0 and cone signals, since we have shown that these are roughly in phase at this frequency; but it could arise, as we have suggested in discussing our rod modulation sensitivity data, from a partial cancellation of π_0 signals (or possibly cone signals) by π_0'.

"Sub-threshold" rod and cone effects

Under some conditions, it is possible to make rod–cone phase settings at scotopic modulations that are slightly below the conventionally-obtained threshold—and, indeed, we took advantage of this in extending our phase measurements beyond the c.f.f.'s suggested by our threshold measurements (compare the highest frequencies shown in Figs 5 and 7, for example). This difference in rod sensitivity for the two tasks is undoubtedly related to the differences between the tasks themselves. In setting phase, the subject is able to compare the flicker amplitude produced by in-phase and opposite-phase combination of a suprathreshold cone signal with a (perhaps subthreshold) rod signal. Setting a rod–cone phase lag, therefore, can be thought of as a discrimination task in the presence of a pedestal—a task that is quite distinct from the simple detection task.

If rod signals that are below the conventional modulation threshold can be used to make phase settings, then it is likely too that small sub-threshold cone signals can also be used. In our experiments, small sub-threshold cone signals are likely to be produced by the 500 nm light used as the rod stimulus for making rod–cone phase settings, even though the 500 nm flicker is below the conventional threshold measured during the cone plateau of dark adaptation. The effect of such sub-threshold cone intrusion should be to cause the phase delays to deviate towards 0° (or towards 360°). The absence of any such large deviations of this type in our rod data, suggests that the sub-threshold cone signals must be quite small compared to the stronger and supra-threshold rod signals. If sub-threshold cone signals do have an effect on phase, it is reasonable to assume that their effects will be most evident under conditions where the rod signal is very small: such as when π_0 and π_0' signals are in opposite phase and cancel each other, or at high frequencies near the limits of rod detection. One condition where such cone distortion could be important is during the rapid transition from π_0' to π_0 found with increasing flicker frequency at intermediate scotopic adaptation levels (triangles, Figs 6, 7 and 8). During this transition, cancellation between π_0' and π_0 may increase the relative prominence of the sub-threshold cone signals, the effect of which should be to accelerate the phase transition towards 360°. This interpretation is consistent with the shallower transition found when cone detection of the 500 nm rod stimulus is further disfavored by using the Stiles–Crawford effect (inverted triangles, Fig. 8). Another condition where cone distortion might be important is during the initial change in phase seen below 0.5 scotopic td in the 20 Hz data of Fig. 9 (diamonds). Sub-threshold cone effects are an attractive explanation of the 20 Hz data, since the transition from 450 to 180° is too large and in the wrong direction to be explained by a simple transition from π_0 to π_0'. With just two processes the transition should have been through 90°, the shortest phase angle between 450 and 180°—not through 270° as our data show (since phase angle is cyclical the transition from 450 to 180° should appear similar to one from 90 (450 – 360) to 180°). The 270° transition in our data may reflect two transitions: one between π_0 and the cones (450–360°) and a second between the cones and π_0' (360–180°).

Phase characteristics

It is surprising to find such large phase differences between signals that show quite similar modulation sensitivity as a function of frequency. Indeed, as inspection of Fig. 5 reveals, when π_0 and π_0' are tested at comparable adaptation levels (circles and triangles) the slight difference in the modulation sensitivity functions goes in the opposite direction from what would be expected on the basis of their phase characteristics: π_0, which has a much greater phase lag, shows a slightly less steep loss of sensitivity with increasing frequency; and π_0'–π_0 transitions with increasing frequency (Figs 6–8) confirm this. The greater phase lag for π_0 could be accounted for by invoking either an added delay of around 33 msec, or else transmission of the π_0 signal through integrating stages that have time constants too short to have much effect on modulation sensitivity in the observable range. Alternatively, it might be proposed that the differences in phase occur not because there is a great difference in the dynamics of the two systems but because one signal is inverted relative to the other; but this idea can be rejected because it predicts that the phase–frequency curves should have parallel slopes, instead of converging toward zero frequency as they do in Figs 6–8. It also predicts scotopic nulls at low frequencies where they are not observed.

Intensity dependence of the two rod signals

If two independent rod pathways develop signals, with different phase lags, which are reunited and contribute additively to a resultant rod signal, the phase of the resultant will in general vary between that of the two components as stimulus intensity or frequency is varied. The abrupt phase jumps of about 180° that we have noted when passing through the "scotopic null" are consistent with this sort of model. When the two components differ in phase by 180°, the resultant retains the phase of whichever component is larger in amplitude, and as their amplitudes vary through equality, the resultant abruptly undergoes a reversal in polarity (i.e. a 180° phase shift). For this to occur the two signals must differ in their intensity dependence in a direction consistent with the direction of the polarity reversal, but nothing more than that can be inferred about the intensity dependence of the two signals from the phase data. More information about intensity-dependence is implicit in the phase characteristic at 8 Hz as a function of intensity (see Fig. 9). At this frequency the component mechanisms appear to differ in phase by about 90°, with little dependence of either phase on intensity. With a sinusoidal input, then, the signals from π_0 and

π_0' will be in quadrature, with amplitude proportional to their intensity-dependent modulation sensitivities $S(I)$ and $S'(I)$ respectively. If ϕ_0 is the phase lag of the faster π_0' component, the signal formed by summing the two components has a phase lag ϕ of:

$$\phi = \phi_0 + \arctan[S(I)/S'(I)].$$

To obtain ϕ as a function of I, we must know $S(I)$ and $S'(I)$ as functions of intensity; the more different these functions are the more rapidly will ϕ change as intensity changes. Suppose for instance that in the region of the null $S(I)$ is inversely proportional to intensity (Weber's Law), while $S'(I)$ is independent of intensity. With the exponents relating sensitivity to intensity thus differing by one, the predicted resultant rod signal phase lag is simply:

$$\phi = \phi_0 + \arctan(I_0/I);$$

where I_0 is the null intensity at which the two processes are equally sensitive. The cone signal phase required to null the flicker of the rod stimulus should show the same intensity dependence; we here neglect the intensity dependence of the cone system phase lag, which is comparatively slight (Veringa & Roelofs, 1966). However, this prediction is not borne out in Fig. 9: the observed transition in phase lag from π_0 to π_0' at 8 Hz is more rapid than predicted from the above equation, with a steepest gradient of about 140° per log unit instead of the predicted 75°. Moreover, any intensity dependence in the individual phase lags of π_0 and π_0' appears much too small to improve the fit substantially, and the comparatively slight speeding of cone responses at high intensities (Veringa & Roelofs, 1966) works in the wrong direction.

Extending the above calculations, we find that the exponent relating $S(I)$ to intensity must exceed that relating $S'(I)$ to intensity by more than two to adequately describe the abrupt phase change found at 8 Hz. To account for the phase data on the basis of an independent signals model, then, requires that π_0 saturates in the region of most rapid phase change, quite independently of π_0', and far below the normal rod saturating intensity. Some amendment to the scheme involving independent rod processes may be required: one possibility is a mutual suppressive interaction that accentuates the predominance of the more active of the two processes (i.e. a winner-takes-all arrangement). This would accelerate the phase change in the region of the null. The phase lag data at 20 Hz, however, cannot be explained in this way. Here π_0' leads π_0 by more than 180°, so that as π_0' comes into play at the higher intensities its effect should be to progressively retard the resultant signal, rather than to advance it as we observe. To explain this on the "independent signals" model, it might be necessary to assume a very strong intensity-dependence of the π_0' phase at this frequency; cone intrusion is also a possibility at 20 Hz as discussed above.

In any case, it is clear that, for whatever reason, the π_0 and π_0' signals differ very much in their dependence on stimulus intensity.

Adaptation behavior

As the foregoing implies, the two rod mechanisms differ radically in their adaptation behavior. In the intensity range up to 1 scot. td, π_0 sensitivity is regulated largely as if by a simple gain change or response compression, so that the shape of the modulation sensitivity function as well as the phase lags are roughly intensity-invariant, while sensitivity varies roughly in proportion to Weber's Law. In the higher intensity range, our results support those of Conner (1982) is showing a substantial shortfall from Weber's Law at higher flicker frequencies, and a speeding up of the response at high intensities, as reflected in the phase lags and the modulation sensitivites. A plausible conclusion is that the π_0' signal may evade the sensitivity regulating site where π_0 signals are attenuated. This is not unreasonable, since the π_0 sensitivity regulating mechanism is postreceptoral in primates (Rushton, 1965; Baylor, Nunn & Schnapf, 1984; MacLeod, Chen & Crognale, 1984; Sharpe, 1990), and therefore might be bypassed by a π_0' signal that travels through different pathways, for instance through cone pathways. Cone signals speed up with light adaptation (Kelly, 1961; Baylor & Hodgkin, 1974) so π_0' is cone-like in this respect. But its spectral sensitivity to background fields is scotopically dominated, so we cannot assume that π_0' sensitivity is controlled only or even predominantly by cones.

It is important to note that this differential light adaptation of π_0 and π_0' is shown not only by the partial immunity of high frequency flicker to light adaptation, but also by the very existence of a well-defined scotopic null in the 1–2 scot. td intensity range, which requires, as noted above, that the two signals grow in a different way with increasing intensity at a fixed frequency such as 15 Hz.

Anatomical basis of the mechanisms

For the physical substrate for the two putative rod processes, it is not necessary to invoke the existence of two types of rod photo-receptors, as has been done (with no strong justification) to explain the threshold data of typical, complete achromats or rod monochromats (Hecht et al., 1948; Lewis & Mandelbaum, 1943; Sloan, 1954, 1968). (For a review of this literature, see Norby & Sharpe, 1988; Sharpe & Nordby, 1990). Only in the all-rod skate retina (Green & Siegel, 1975) is there any indication of such a duality at the receptor level.

Models in which the two signals coexist within a single rod, and contribute to its hyperpolarization by light, have the virtue of accounting easily for the psychophysical flicker null, which requires that the signals ultimately converge. These models, however, cannot account for the differences between π_0 and π_0' in light adaptation: since light adaptation does not take place within primate rods, but postreceptorally, the signals from the two processes must be conveyed by separate pathways through some stage or stages at which light adaptation occurs, before being later recombined.

The first pathway, associated with the π_0 process, is probably controlled exclusively by rods. Its signals most likely pass through the rod-only bipolar cells, which have been identified by y Cajal (1893, 1933) in a number of vertebrate species and by Polyak (1941), Boycott and Dowling (1969) and Kolb (1970) in primates. It is an attractive speculation that the second pathway, associated with the π_0' process, may combine signals from rods and cones. The rod and cone systems have, in fact, been often demonstrated psychophysically to interact in various ways (see, for instance, Willmer, 1950; McCann & Benton, 1969; Makous & Boothe, 1974; Frumkes, Sekuler & Reiss, 1972; Buck, Peoples & Makous, 1979; Buck, Berger & Cook, 1984; D'Zmura & Lennie, 1986; Sharpe, Fach, Nordby & Stockman, 1989). Further, there is much anatomical and some physiological evidence for the convergence of rod and cone signals on to retinal interneurones in the mudpuppy (Fain, 1975; Fain & Dowling, 1973), tiger salamander (Lasansky, 1973), cat (Kolb & Famiglietti, 1974) and monkey (Hubel & Wiesel, 1960; Gouras, 1965, 1967; Gouras & Link, 1966; Kolb, 1970). In the cat, rod signals even enter the cones themselves (Nelson, 1977). The threshold for observation of a rod signal in the cat cone pathway is about 7 quanta absorbed/rod/sec (Nelson, 1977); a similar value emerges from modelling of the network of rod–rod and rod–cone gap junctions (Smith, Freed & Sterling, 1986). This corresponds to about 1 scot. td, the intensity at which π_0' first reveals itself psychophysically.

A rod signal that travels postreceptorally through cone pathways might well be more cone-like in its characteristics as a result. Temporal resolution in particular might be improved, since Baylor and Fettiplace (1976) have shown that the pathways from the cones to the ganglion cells in turtle are faster than the pathways from the rods to the same ganglion cell. This model places the π_0/π_0' bifurcation immediately after the rods themselves. But our efforts to demonstrate a special relationship between π_0' and cones (see bipartite field observations, above) provide only weak support for this cone pathway model, particularly in light of our finding (and that of Conner, 1982, Fig. 4) that the field sensitivity of π_0' is rod dominated.

Another possibility is that π_0' signals pass through an interneuron similar in function to the AII amacrine cell found in the cat retina (Nelson, 1982); which may correspond morphologically to amacrine cell type A6 in the rhesus monkey (Mariani, 1988). Amacrine cells of this type are mainly driven by rods, with a tiny response component coming from the long-wavelength sensitive cones. Their function seems to be to quicken the time course of the sluggish signals while keeping those signals well localised in space. The addition of this cell in one of the rod pathways may provide, as Nelson speculates, a significant improvement in the speed of perception for small luminous objects on scotopic backgrounds. If this is so, however, it is surprising that π_0' does not differ from π_0 in its spatial characteristics (see Bipartite field observations, above), as well as in its temporal and adaptational behaviour. Moreover the physiological threshold intensity of AII amacrines is some twenty five times lower than that of π_0' (Nelson, 1982).

A third possibility is the biplexiform cell that has been identified in the Rhesus monkey (Mariani, 1982; Zrenner, Nelson & Mariani, 1983). This cell type constitutes approximately 2% of all ganglion cells found in the monkey retina. In addition to dendritic processes that are postsynaptic to amacrine and bipolar cells in the inner plexiform layer, each biplexiform cell has a long dendritic process that bypasses bipolar cells and directly contacts rods. Since a part of their input circumvents the usual interneuronal circuitry of the retina, it is possible that such cells could transmit scotopic signals to the brain more rapidly than the other types of retinal ganglion cells.

Acknowledgements—This work was supported by NSF grant BNS 86-09217 and NIH grant EY01711. LTS's visits to the UCSD Vision Laboratory were made possible by a fellowship and travel funds awarded to him by the Alexander von Humboldt Foundation (Bonn–Bad Godesberg) and by funds received from the Deutsche Forschungsgemeinschaft (Bonn) SFB 325, Teilprojekt B-4. We are grateful to John Mollon and Ethan Montag for comments.

REFERENCES

Aguilar, M. & Stiles, W. S. (1954). Saturation of the rod mechanism of the retina at high levels of stimulation. *Optica Acta, 1*, 59–65.

Alpern, M., Falls, H. F. & Lee, G. B. (1960). The enigma of typical total monochromacy. *American Journal of Opthalamology, 50*, 996–1012.

Arden, G. B. & Weale, R. A. (1954). Variations in the latent period of vision. *Proceedings of the Royal Society, London, B142*, 258–269.

Baylor, D. A. & Fettiplace, R. (1976). Transmission of signals from photoreceptors to ganglion cells in the eye of the turtle. *Cold Spring Harbor Symposiums on Quantative Biology, 40*, 529–536.

Baylor, D. A. & Hodgkin, A. L. (1974). Changes in time scale and sensitivity in turtle photoreceptors. *Journal of Physiology, London, 242*, 729–758.

Baylor, D. A., Nunn, B. J. & Schnapf, J. L. (1984). The photocurrent, noise and spectral sensitivity of the rods of the monkey *Macaca fascicularis. Journal of Physiology, London, 357*, 575–588.

van den Berg, T. J. T. P. & Spekreijse, H. (1977). Interaction between rod and cone signals studied with temporal sine wave stimulation. *Journal of the Optical Society of America, 67*, 1210–1217.

Blakemore, C. B. & Rushton, W. A. H. (1965). Dark adaptation and increment threshold in a rod monochromat. *Journal of Physiology, London, 181*, 612–628.

Boycott, B. B. & Dowling, J. E. (1969). Organisation of the primate retina: Light microscopy. *Philosophical Transactions of the Royal Society, 255*, 109–184.

Brooke, R. T. (1951). The variation of critical fusion frequency with brightness at various retinal locations. *Journal of the Optical Society of America, 41*, 1010–1016.

Buck, S. L., Berger, A. & Cook, J. (1984). Rod–cone interactions: effects of test size, duration and eccentricity. *Journal of the Optical Society of America, A1*(12), 1327*A*.

Buck, S. L., Peeples, D. R. & Makous, W. (1979). Spatial patterns of rod–cone interaction. *Vision Research, 19*, 775–782.

y Cajal, S. R. (1893). The vertebrate retina (translated by Maguire, D. and Rodieck, R. W.). In Rodieck, R. W. (Ed.), *The vertebrate retina: Principles of structure and function*, Appendix I (1973). San Francisco: W. H. Freeman.

y Cajal, S. R. (1933). La rétine des vertébrés. *Trabajos del Labaratorio de investigaciones bioquimicas de la Universidad de Madrid, 28*, 1–141. (Appendix to Vol. 28).

Conner, J. D. (1982). The temporal properties of rod vision. *Journal of Physiology, London, 332*, 139–155.

Conner, J. D. & MacLeod, D. I. A. (1977). Rod photoreceptors detect rapid flicker. *Science, Washington, 195*, 689–699.

D'Zmura, M. & Lennie, P. (1986). Shared pathways for rod and cone vision. *Vision Research, 26*, 1273–1280.

Fain, G. L. (1975). Interactions of rod and cone signals in the mudpuppy retina. *Journal of Physiology, London, 252*, 735–769.

Fain, G. L. & Dowling, J. E. (1973). Intracellular recordings from single rods and cones in the mudpuppy retina. *Science, Washington, 180*, 1178–1181.

Frumkes, T. E., Sekuler, M. D. & Reiss, E. H. (1972). Rod–cone interactions in human scotopic vision. *Science, Washington, 175*, 913–914.

Gouras, P. (1965). Primate retina: duplex function of dark adapted retinal ganglion cells. *Science, Washington 147*, 1593–1594.

Gouras, P. (1967). The effects of light-adaptation on rod and cone receptive field organization of monkey ganglion cells. *Journal of Physiology, London, 192*, 747–760.

Gouras, P. & Gunkel, R. D. (1964). The frequency response of normal, rod monochromat and nyctalope ERG's to sinusoidal monochromatic light stimulation. *Documenta Opthalmologica, 18*, 137–150.

Gouras, P. & Link, K. (1966). Rod and cone interaction in dark-adapted monkey ganglion cells. *Journal of Physiology, London, 184*, 499–510.

Green, F. G. & Siegel, I. M. (1975). Double branch flicker curves from the all-rod skate retina. *Science, Washington, 188*, 1120–1122.

Hallett, P. E. (1962). Scotopic acuity and absolute threshold in brief flashes. *Journal of Physiology London, 163*, 175–189.

Hecht, S., Shlaer, S., Smith, E. L., Haig, C. & Peskin, J. C. (1948). The visual functions of the complete color-blind. *Journal of General Physiology, 31*, 459–472.

Hess, R. F. & Nordby, K. (1986). Spatial and temporal limits of vision on the achromat. *Journal of Physiology London, 371*, 365–385.

Hubel, D. H. & Wiesel, T. N. (1960). Receptive fields of optic nerve fibers in the spider monkey. *Journal of Physiology London, 154*, 572–580.

Ives, H. E. (1922). Critical frequency relations in scotopic vision. *Journal of the Optical Society of America and Review of Scientific Instruments, 6*, 254–268.

Kelly, D. H. (1961). Visual responses to time-dependent stimuli. I. Amplitude sensitivity measurements. *Journal of the Optical Society of America, 51*, 422–429.

Kelly, D. H. (1972). Flicker. In Jameson, D. & Hurvich, L. M. (Eds.), *Handbook of sensory physiology* (Vol. VII/4). New York: Springer.

Kohlrausch, A. (1922). Untersuchungen mit farbigen Schwellenprüflichtern über den Dunkelnadaptationsverlauf des normalen Auges. *Pflügers Archiv für die gesamte Physiologie, 196*, 113–117.

Kolb, H. (1970). Organization of the outer plexiform layer of the primate retina: Electron microscopy of Golgi-impregnated cells. *Philosophical Transactions of the Royal Society, London, B258*, 261–283.

Kolb, H. & Famiglietti, E. V. (1974). Rod and cone pathways in the inner plexiform layer of the cat retina. *Science, Washington, 186,* 47–49.

von Kries, J. (1894). *Bericht der Naturforschung Gesellschaft zu Freiburg im Breisgau IX (2),* p. 61.

Lasansky, A. (1973). Organization of the outer synaptic layer in the retina of the larval tiger salamander. *Philosophical Transactions of the Royal Society, London, B265,* 471–489.

Lewis, S. D. & Mandelbaum, J. (1943). Achromatopsia: Report of three cases. *Archiv Ophthalmalogica, 30,* 225–231.

MacLeod, D. I. A. (1972). Rods cancel cones in flicker. *Nature, London, 235,* 173–174.

MacLeod, D. I. A. (1974). Signals from rods and cones. Ph.D. dissertation. University of Cambridge.

MacLeod, D. I. A., Chen, B. & Crognale, M. (1984). Local adaptation vs. neural pools in rod vision. *Investigative Ophthalmology and Visual Science* (Suppl.), *25,* 53.

Makous, W. & Boothe, R. (1974). Cones block signals from rods. *Vision Research, 14,* 285–294.

Mariani, A. P. (1982). Biplexiform cells: ganglion cells of the retina that contact photoreceptors. *Science, Washington, 216,* 1134–1136.

Mariani, A. P. (1988). Amacrine cells of the rhesus monkey retina. *Investigative Opthalmology and Visual Science* (Suppl.), *29,* 128.

McCann, J. J. & Benton, J. L. (1969). Interaction of the long-wave cones and the rods to produce color sensations. *Journal of the Optical Society of America, 59,* 103–107.

Nelson, R. (1977). Cat cones have rod input: A comparison of the response properties of cones and horizontal cell bodies in the retina of the cat. *Journal of Comparative Neurology, 172,* 107–135.

Nelson, R. (1982). AII amacrine cells quicken time course of rod signals in the cat retina. *Journal of Neurophysiology, 47,* 928–947.

Nordby, K. & Sharpe, L. T. (1988). The directional sensitivity of the photoreceptors in the human achromat. *Journal of Physiology London, 399,* 267–281.

Polyak, S. L. (1941). *The retina.* Chicago: University of Chicago Press.

Rushton, W. A. H. (1965). The Ferrier lecture, 1962: Visual adaptation. *Proceedings of the Royal Society, London, B162,* 20–46.

Sharpe, L. T. (1990). The light-adaptation of the rod visual system. In Hess, R., Sharpe, L. T. & Nordby, K. (Eds.), *Night vision: Basic, clinical and applied aspects.* Cambridge: Cambridge University Press.

Sharpe, L. T., Fach, C. C., Nordby, K. & Stockman, A. (1989). The rod increment threshold and Weber's Law. *Science, Washington, 244,* 354–356.

Sharpe, L. T. & Nordby, K. (1990). The photoreceptors in the achromat. In Hess, R. F., Sharpe, L. T. & Nordby, K. (Eds.), *Night vision: Basic, clinical and applied aspects.* Cambridge: Cambridge University Press.

Shlaer, S. (1937). The relation between visual acuity and illumination. *Journal of General Physiology, 21,* 165–168.

Sloan, L. L. (1954). Congenital achromatopsia: a report of 19 cases. *Journal of the Optical Society of America, 44,* 117–128.

Sloan, L. L. (1958). The photopic retinal receptors of the typical achromat. *American Journal of Opthalmology, 46,* 81–86.

Smith, R. G., Freed, M. A. & Sterling, P. (1986). Microcircuitry of the dark-adapted cat retina: Functional architecture of the rod–cone network. *Journal of Neuroscience, 6,* 3505–3517.

Stiles, W. S. (1939). The directional sensitivity of the retina and the spectral sensitivities of the rods and cones. *Proceedings of the Royal Society, London, B127,* 64–105.

Stiles, W. S. (1959). Color vision: The approach through increment-threshold sensitivity. *Proceedings of the National Academy of Sciences, U.S.A., 45,* 100–114.

Stiles, W. S. & Crawford, B. H. (1934). The liminal brightness increment for white light for different conditions of the foveal and parafoveal retina. *Proceedings of the Royal Society, B116,* 55–102.

Stockman, A., MacLeod, D. I. A. & Depriest, D. D. (1989). The temporal properties of the human short-wave photoreceptors and their associated pathways. *Vision Research* (in press).

Stockman, A., Sharpe, L. T., Fach, C. & Nordby, K. (1989). Rod flicker perception: scotopic duality in the typical, complete achromat (submitted).

Veringa, F. & Roelofs, J. (1966). Electro-optical stimulation in the human retina. *Nature, London, 211,* 321–322.

Wald, G. (1945). Human color vision and the spectrum. *Science, New York, 101,* 653–658.

Walls, G. L. & Heath, G. G. (1954). Typical total color blindness reinterpreted. *Acta Ophthalmologica, 32,* 253–297.

Willmer, E. N. (1950). Low threshold rods and the perception of blue. *Journal of Physiology London, 111,* 17P.

Wyszecki, G. & Stiles, W. S. (1982). *Color science, concepts and methods, quantitative data and formulas* (2nd edn). Wiley: New York.

Zrenner, E., Nelson, R. & Mariani, A. (1983). Intracellular recordings from a biplexiform ganglion cell in macaque retina stained with horseradish peroxidase. *Brain Research, 262,* 181–185.